Available online at www.sciencedirect.com

ScienceDirect

Procedia: Editor

Procedia

www.elsevier.com/locate/procedia

Simple drag prediction strategies for an Autonomous Underwater Vehicle's hull shape

Pareecha Rattanasiri[a,*], Philip A. Wilson[b], Alexander B. Phillips[c]

[a]*Department of Mechanical Engineering, Faculty of Engineering, Burapha University,Chonburi 2013,1 Thailand*
[b,c]*Fulid Structure Interactons Group, Engineering and the Environment, University of Southampton, Southampton SO16 7QF, United Kingdom*

Abstract

The range of an AUV is dictated by its finite energy source and minimising the energy consumption is required to maximise its endurance. One option to extend the endurance is by obtaining the optimum hydrodynamic hull shape with balancing the trade-off between computational cost and fluid dynamic fidelity. An AUV hull form has been optimised to obtain low resistance hull. Hydrodynamic optimisation of hull form has been carried out by employing five parametric geometry models with a streamlined constraint. Three Genetic Algorithm optimisation procedures are applied by three simple drag predictions which are based on the potential flow method. The results highlight the effectiveness of considering the proposed hull shape optimisation procedure for the early stage of AUV hull design.

Keywords: Type your keywords here, separated by semicolons ;

1. Introduction

The power required to overcome hydrodynamic drag is an important component of the energy budget of Autonomous Underwater Vehicles. The drag experienced by the vessel is a direct consequence of the hull shape and operating speed of the vehicle. Various AUV's shapes have been developed, ranging from: the conventional torpedo shape (e.g. Autosub), streamlined shapes (e.g. REMUS 100) and multi-hull vehicles (e.g. DeepC, ABE). Often the primary driver in the hull shape of the vehicle is not minimising the drag per unit volume; other constraints such as: pressure vessel selection, launch mechanism, available deck area, container size, etc take priority.

In 1974, the first optimisation AUV hull shape was performed by Parsons et al. (1974) by using a direct optimisation strategy where the body geometry and the hydrodynamic shape is defined by a set of mathematical formulae, the unknown variables as a function of the body geometry had been randomly selected, then the hydrodynamic drag of that body was predicted, finally a black box optimisation procedure was used to define the minimum total drag hull. Additional optimisation approaches have been proposed by (Myring, 1976; Zedan and Dalton, 1986). Alternatively, hull shapes can be designed by employing trial and error techniques or the designer's experience with the use of drag prediction simulations (Huggins and Packwood, 1994; Sarkar et al., 1997; Rutherford and Doerffela, 2005; Stevenson et al., 2007; Jagadeesh et al., 2009; Karim et al., 2009; Husaini et al., 2009). More recently, high performance computers and Computational Fluid Dynamic (CFD) using Reynolds

* Corresponding author. Tel.: +66 92 768 7904; fax: +66 3839 0351
E-mail address: pareecha@eng.buu.ac.th, pj506@soton.ac.uk

Averaged Navier- Stoke (RANS) simulation techniques for predicting the hull drag have become the conventional tools for AUV designers (Phillips et al., 2010; Jagadeesh et al., 2009; Karim et al., 2009; Phillips et al., 2008, 2007; Sarkar et al., 1997; Rattanasiri et al., 2013c,b,a).

The aims of this study are, firstly, to develop three simple drag prediction strategies for an AUV hull suitable for hull shape optimization, secondly, to develop simple optimisation procedures using the commercial MATLAB optimisation toolbox. The drag prediction strategies range in complexity from a purely empirical approach, a basic potential flow approach through to a potential flow approach with separation prediction. RANS-SST simulation, are used to validate the results with the first three drag strategies.

2. Mathematical hull geometries

This work assumes a length Reynolds number (*ReL*) 2.85 × 10^6. To define the mathematical shape of the vehicle two streamlined curve equations are considered; the ellipsoid curve and the sectional-area curve (Landweber and Gertler, 1950; Rattanasiri and Wilson, 2010).

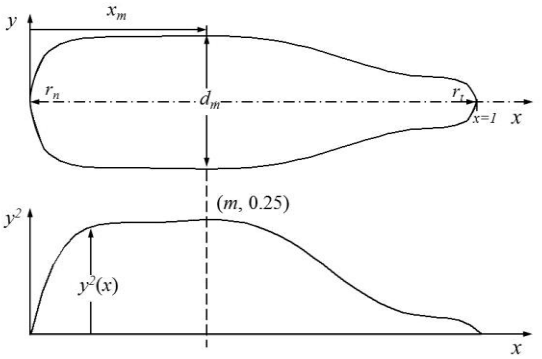

Figure 1: Sketches of (top) a body of revolution ($y(x)$) and (bottom) a sectional-area curve ($y^2(x)$)

2.1. Sectional-area curve hull

Sectional-area curve is a single set of mathematical line equation that can generate various curvatures. Sketches of two-dimensional shape of body of revolution (y) and its sectional-area curve (y^2) in dimensionless form (Landweber and Gertler, 1950; Rattanasiri and Wilson, 2010) show in Figure 2. Where m is the position of maximum radius of area curve, Cp is the prismatic coefficient; rn is the radius of curvature at nose and rt the radius of curvature at tail.

3. Numerical approaches

Fluids in motion are subject to the normal stress (or pressure) and tangential shear stress, for air, water, and other engineering fluids, shear stresses can be related to the velocity field. The momentum conservation principle for such fluids is expressed by the Navier-Stokes equations. Assuming this AUV is fully submerged in deep water, there will be no wave resistance, the total drag coefficient; C_D based on the wetted surface area is therefore only due to the viscous drag (C_v) and can be estimated as:-

$$C_D = C_v = (1+k)C_F = Drag/(0.5\rho V^2 A_w) \tag{7}$$

Where C_F is the skin friction drag. The total drag coefficient based on the volumetric C_{DV} can be estimated as:-

$$C_{DV} = C_D \frac{A_w}{\nabla^{2/3}} = Drag/(0.5\rho\nabla^{2/3}V^2) \tag{8}$$

Where ρ is the fluid density, A_w is the wetted surface area and V is the fluid velocity.

3.1. Drag prediction strategy

The drag prediction strategies utilised in this study are summarised as following:-

3.1.1 Drag prediction strategy 1 (fully empirical)

The simplest drag prediction strategy is fully empirical; the total drag coefficient is calculated from a prediction of the viscous drag coefficient. The skin friction coefficient; $(C_F)_{1957}$ obtained by the ITTC'57 ship correlation line (ITTC, 1957) as a function of Reynolds number (*Re*) where A_W is the wetted surface area and *V* is the vehicle speed:-

$$(C_F)_{1957} = \frac{0.075}{(\log_{10}(\mathrm{Re}) - 2)^2}, \tag{9}$$

and the form factor (1+k) (Hoerner, 1965) in term of hull length (*L*) and maximum hull diameter (d_M):-

$$(1+k) = 1 + 1.5(d_m / L)^{3/2} + 7(d_m / L)^3 \tag{10}$$

3.1.2 Drag prediction strategy 2 (semi-empirical)

The second drag prediction strategy is based on potential flow. Utilising Schlichting's C_F prediction ($C_{F,Schlichting}$) (Schlichting, 1962), this study selects the solution of a Fredholm integral equation developed by Landweber (1959) to predict the tangential local velocity (u_e) and the local Reynolds number $\left(\mathrm{Re}_{sch} = \frac{|U_\infty| s}{\nu}\right)$ on the surface by neglecting the change in pressure force due to viscous effect.

$$\begin{aligned} C_{F,Schlichting} &= 0.664\ \mathrm{Re}_{sch}^{-0.5} && \text{for} \quad \mathrm{Re}_{sch} < 3\times10^5 \\ C_{F,Schlichting} &= 0.074\ \mathrm{Re}_{sch}^{-0.2} - 1050\ \mathrm{Re}_{sch}^{-1} && \text{for} \quad 3\times10^5 < \mathrm{Re}_{sch} < 1\times10^7 \end{aligned} \tag{11}$$

where s is the distance to the leading edge.

3.1.3 Drag prediction strategy 3 (numerical)

The third method uses potential flow and a classical boundary layer method. The local velocity (u_e) is determined by the Fredholm integral solution for a given free stream velocity (Landweber, 1959). The boundary layer method to predict the skin friction drag was introduced by Moran (1984); the C_F from laminar boundary layer growth is predicted by using Thwaites' method, the skin friction coefficient (C_F) are then predicted from the semi-empirical formulas given by Cebeci and Bradshaw (1977). Laminar separation criteria is set where the wall shear stress drop to zero, $\lambda < -0.0842$. Transition point is predicted using Michel's criterion. Turbulent separation is predicted when the shape factor (*H*) reaches the value 2.4. If no laminar or turbulent separation occurs, the Ludwieg-Tillman skin-friction drag can be calculated (White, 1974).

3.1.3 Reynolds Averaged Navier Stokes (RANS) simulation (numerical)

To provide insights into the behaviour of the presiding drag prediction strategies several validation cases have also been performed using the more advanced RANS CFD methodology. The SST turbulence models are chosen with the transition package; fully turbulent turbulence model, $\gamma - \theta$ model and $\gamma - \theta$ fixed transition model, provided by ANSYS CFX 12.1. The computational parameters are provided in Table 1. The model domain, boundary condition

and mesh strategies used in this simulation are the same strategy as shown in reference Rattanasiri et al. (2012, 2013c,b,a).

3.2. Validation drag prediction strategies

The experimental data of Series 58 (Gertler, 1950) including the numerical data are selected for comparison with the drag prediction strategies. Figure 4(a) illustrates the drag predictions for a range of fineness ratios compared with the experimental results (Gertler, 1950) and previous CFD simulations (Nakayama and Patel, 1973). The experimental and numerical results as well as the first two drag prediction strategies illustrate an optimum fineness ratio for minimal volumetric drag at a fineness ratio of about 5. However drag prediction strategy three predicts an optimum at a fineness ratio of four.

The influence of Reynolds number on volumetric drag coefficient is illustrated in Figure 4(b). Drag prediction strategy 3 is not predicting assuming delayed transition and consequently the drag result is less than the other results. The total drag is over predicted by 7.5%, 7.2% and 4.2% by drag prediction strategies 1, 2 and 4, compared to the experimental results. Whilst the total drag is under predicted approximately 45.5% by drag prediction strategy 3 due to the early predicted transition point.

To The difference between the drag prediction strategies can be explained by examining the skin friction distribution along the vessel. Agreement between the experiment and the Fredholm integral model is satisfactory over 90% of the body surface from the nose. For the three different drag prediction strategies; drag prediction strategy 1 is the estimation of an average value of the skin friction drag with depend upon the Re_L, thus it cannot be evaluated. The results from RANS-SST fully turbulent model, RANS-SST $R-\theta$ turbulent model (fixed transition point at 27.5%L from the nose) and RANS-SST $R-\theta$ turbulent model is demonstrated in Figure 5 by the black line, orange line and green line, respectively. The results illustrate that by improving the transition model of drag prediction strategies 2 and 3, the more accurate results could be obtained for the optimisation procedure.

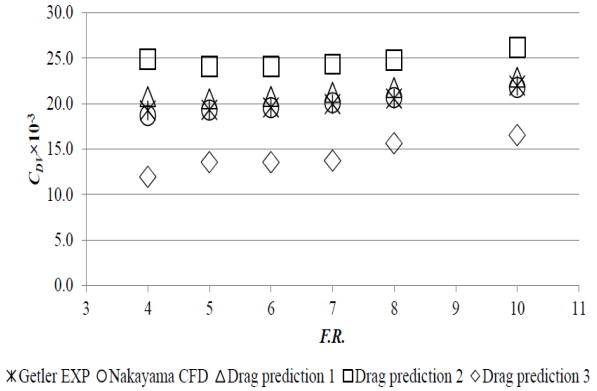

a) Fineness ratio (*F.R.*)

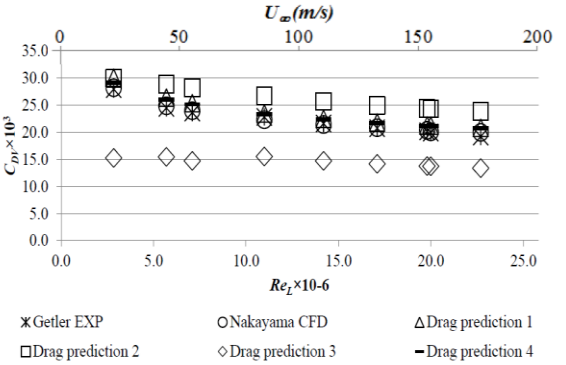

B) Re_L

Figure 4: Comparison of the drag of Series 58 between experimental data (Gertler, 1950), Nakayama and Patel (1973)'s calculation and drag prediction strategies (a) at various *F.R.* at $\mathrm{Re}_L = 20 \times 10^6$ (b) at various Re_L at F.R.=7.0

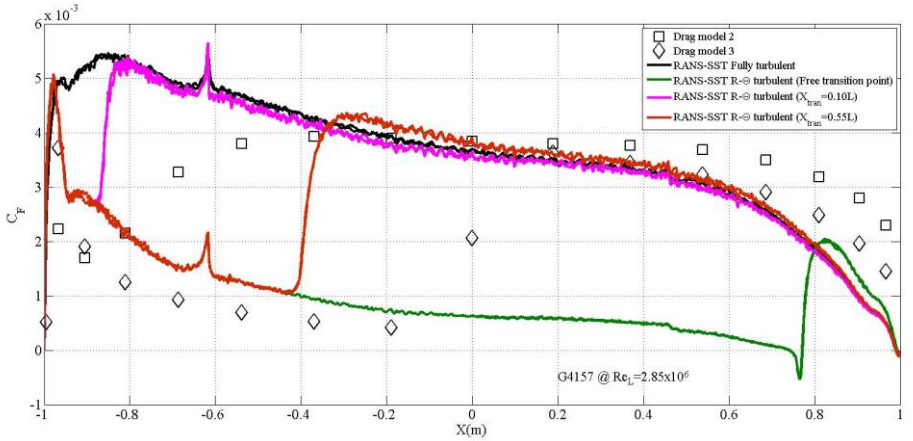

Figure 5: Comparison the skin friction distributions from drag prediction strategy 2 and drag prediction strategy 3 with the results from drag prediction strategy 4 RANS-SST simulation of G4157 at $\mathrm{Re}_L = 2.85 \times 10^6$

4. MATLAB GA Optimisation strategy

For optimisation procedure, the objective function is used to provide a measure of how individuals have performed in the problem domain. For a minimisation problem, the fit individuals will have the lowest numerical value of the associated objective function, in this study; this is the total volumetric drag coefficient. The objective function is:-

$$C_{DV} = (1+k)\frac{A_w}{\nabla^{2/3}} = Drag/(0.5\rho\nabla^{2/3}V^2) \tag{12}$$

25 optimisations were performed for each case. The best result of the population diversity, the setup of GA options is selected as following: Generations = 100, Populations = 200, Crossover fraction = 0.8, Selection = Stochastic Function, Elite count = 2.0.

5. AUV hull shape optimisation

5.1. Streamlined hull shape results

Streamlined hull shape results of optimisation strategy 1, 2 and 3 are shown in Figure 10. The results show that:-

- Four types of local optimal shape; Stern shape, Bow shape, Hill shape and Cylinder shape, are obtained by the optimisation strategies 1 and 2.
- The shape results from optimisation strategies 3 are constrained by the boundary layer method thus the only streamlined shapes of Stern and Cylinder are obtained.
- It could be highlighted that there are various optimal shapes to be selected at the same minimum hull drag obtained by each optimisation strategy.

6. Conclusion

In order, to optimise a AUV hull to obtain a low resistance hull, three drag strategies are developed. These strategies are then joined to a Genetic Algorithm (GA) within the MATLAB optimisation toolbox to develop three shape optimisation procedures.

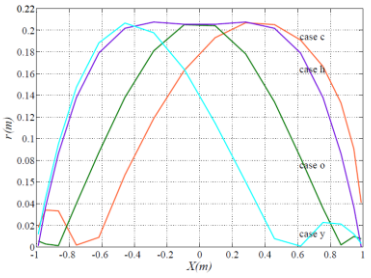

(a) drag prediction strategy 1; Stern shape (case c), Bow shape (case y), Hill shape (case o) and Cylinder shape (case h)

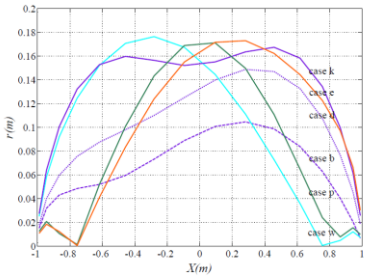

(b) drag prediction strategy 2; Stern shape (case e), Bow shape (case w), Hill shape (case p) and Cylinder shape (case k).

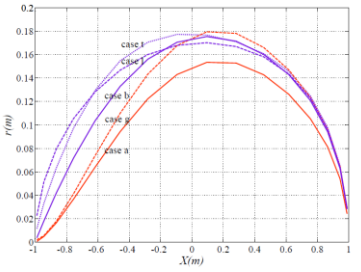

(c) drag prediction strategy 3; Stern shape (case a, g) and Cylinder shape (case b, l and t)

Figure 10: The optimal shape from the drag prediction strategy 1, 2 and 3

Drag prediction strategy 1 (fully empirical) is the simplest drag prediction strategy based on the ITTC'57 skin friction line; it provides the cheapest numerical cost with the lowest fidelity. Drag prediction strategy 2 (semi-empirical) is more complicated drag prediction strategy, the technique couples the potential flow method, Fredholm integral equations, with the Schlichting predictions of skin friction; it provides a moderate numerical cost, with a higher fidelity understanding of the flow. Drag prediction strategy 3 (Numerical) is a viscous drag prediction strategy which utilises a potential flow method as a starting point. The model has a higher computational cost; however local flow conditions and separation can be predicted. Full RANS CFD simulations are also utilised to validate the drag models.

The optimisation strategy applied to the three simple drag prediction strategies described earlier. Each GA MATLAB algorithm is selected with the feasible set-up of Mutation, Generations, Populations and Reproduction i.e. Selection, Elite count and Crossover fraction. Each optimisation strategy has been carried out by employing two parametric curves; ellipsoid curve and the sectional-area curve. Each procedure is validated for the effectiveness of the proposed hydrodynamic optimisation by employing parametric ellipsoid curve. Five parametric geometry models of the sectional-area curve are selected as its streamlined constraint accounts for hull shape variations. 25 optimisations of each strategy have been performed at the Reynolds Number 2.85×10^6.

The results of shape with inflection points from optimisation strategies 1 and 2 are due to the lack of the streamlined constraint. The envelope technique could be applied to the sectional-area curve equation to constraint these strategies, the results may be improved with the cheap computational cost than that of optimisation strategy 3. The results of optimisation strategy 3 are Stern shape and Cylinder shape, these shapes obtained at the same total drag with a similar stern's curve, however, different bow's curve. The transition model is fixed with the transition point of the shape at 0.5L; the results suggest the lower drag shape may be obtained from the different and more accurate transition prediction models. These results suggested a variety of AUV hull shapes from three simple shape optimisation strategies and it could be beneficial to the AUV hull designer.

The study shows that the success of a shape optimisation task depends on a number of important issues. A first important requirement is the capability to generate smooth hull shape variants by varying a number of suitably selected form points. This is actually the key point to be cared for to make design optimisation a fast and reliable process. Since sectional-area curve mathematical model is automatically generated via the optimisation process for streamline to satisfy the given requirements, a fair curve is always generated even with a few subset of parameters unavailable to satisfy the given requirements i.e. rn, rt. The curve can, therefore, be easily used in the AUV hull shape optimisation.

Another important aspect is the selection of the right optimisation criteria, which must take into account of the goal of the optimisation task, but also the features, capabilities and limitations of the CFD tools used to simulate hulls' hydrodynamics. Despite its simplicity, these optimisation procedures can be successfully applied to optimise the shapes of the AUV hull for the low resistance design. This procedure can be used literary effective at the early design stage instead of the trial and error. However, with the improvement of the optimisation procedure such as addition of hull volumetric constraint or the one inflection point constraint, the unique optimal hull shape may be obtained.

7. Future work

Three drag prediction optimisation procedures discussed in this work provides similar hull shape diameter. With the streamlined shape constraint applied to optimisation strategies 1 and 2, these two strategies could provide streamlined shape with the cheap computational cost. With a more accurate transition prediction, the drag prediction strategy 3 could provide more accurate results, consequently, a good streamlined hull shape. By applying the volume constraint to the optimisation process, a unique optimal hull shape may be obtained.

8. Acknowledgement

The authors acknowledge the use of the IRIDIS High Performance Computing Facility, and associated support services at the University of Southampton, in the completion of this work. The work presented in this paper was financed by the Royal Thai Government.

References

1. ANSYS, 2010. ANSYS CFX, Release 12.1. ANSYS.
2. Cebeci, T., Bradshaw, P., 1977. Momentum transfer in boundary layers. Hemisphere Publishing Corporation.
3. Gertler, M., April 1950. Resistance experiments on a systematic series of streamlined bodies of revolution– for application to the design of high speed submarine. Tech. Rep. C-297, David Taylor Model Basin, Naval Ship Research and Development Center, Washington 7, D.C.
4. Hoerner, S. F., 1965. Fluid-dynamic drag: practical information on aerodynamic drag and hydrodynamic resistance. (pubished by the author).
5. Huggins, A., Packwood, A. R., 1994. The optimum dimensions for a long-range, autonomous, deep- driving, underwater vehicle for oceanographic research. Ocean Engineering 21 (1), 45–56.
6. Husaini, M., Samad, Z., Arshad, M. R., 2009. CFD simulation cooperative AUV motion. Indian Journal of marine Sciences 38(3), 346–351.
7. ITTC, 1957. Proceedings of the 8th ITTC, Madrid, Spain. In: Canal de Experiencias Hidrodinamicas, El Pardo, Madrid.
8. Jagadeesh, P., Murali, M., Idichandy, V. G., 2009. Experimental investigation of hydrodynamic force coefficients over AUV hull form. Journal of Ocean Engineering 36, 113–118.
9. Karim, M. M., Rahman, M. M., Alim, M. A., 2009. Computation of turbulent viscous flow around submarine hull using unstructured grid.
10. Landweber, L., 1951. An iteration formula for fredholm integral equations of the first kind. American Journal of Mathematics 73 (3), 615–624.
11. Landweber, L., 1959. Potential flow about bodies of revolution and symmetric two-dimensional flows. Tech. Rep. BuShips Index NS 715-102, Iowa Institute of Hydraulic Research, Iowa City, Iowa.
12. Landweber, L., Gertler, M., Sept 1950. Mathematical formulation of bodies of revolution. Tech. Rep. 719,

Navy Department, The David W. Taylor Model Basin, Washington 7, D.C.

13. Moran, J., 1984. An introduction to theorectical and Computational aerodynamics. McGraw-Hill& Sons, Inc.
14. Myring, D. F., 1976. A theoretical study of body drag in ubcritical axisymmetric flow. The Aeronautical Quarterly, 186–194.
15. Nakayama, A., Patel, V. C., 1973. Calculation of the viscous resistance of bodies of revolution. Journal of Hydronautics 8 (4), 154–162.
16. Parsons, J. S., Goodson, R. E., Goldschmied, F. R., 1974. Shaping of axisymmetric bodies for minimum drag in incompressible flow. Journal of Hydronautics 8, 100–107.
17. Phillips, A., Turnock, S., Furlong, M., 2008. Comparisons of CFD simulations and in-service data for the self-propelled performance of an Autonomous Underwater Vehicle. In: 27th Symposium of Naval Hydrodynamics, Seoul, Korea, 05 - 10 Oct 2008.
18. Phillips, A. B., Furlong, M., Turnock, S. R., 2007. The use of computational fluid dynamics to assess the hull resistance of concept autonomous underwater vehicles. In: OCEANS 2007 - Europe. Richardson TX, USA, Institute of Electrical and Electronics Engineers.
19. Phillips, A. B., Turnock, S. R., Furlong, M., 2010. The use of computational fluid dynamics to aid cost- effective hydrodynamic design of autonomous underwater vehicles. In: Proceedings of the Institution of Mechanical Engineers, Part M: Journal of Engineering for the Maritime Environment. Vol. 224(4). pp. 239–254.
20. Rattanasiri, P., Wilson, P. A., 2010. Mathematical formulation of body of revolution applied to AUV's shape. In: The 3rd International Conference on Underwater System Technology, Malaysia, MY.
21. Rattanasiri, P., Wilson, P. A., Phillips, A. B., 2012. Numerical investigation of the drag of twin prolate spheroid hulls in various longitudinal and transverse configurations. In: AUV2012, Southampton, GB. 24-27 September 2012.
22. Rattanasiri, P., Wilson, P. A., Phillips, A. B., 2013a. Numerical investigation of a fleets of self-propelled A U V s. Submitted (Under review).
23. Rattanasiri, P., Wilson, P. A., Phillips, A. B., 2013b. Numerical investigation of a fleets of towed AUVs. Ocean Engineering 80, 25-35.
24. Rattanasiri, P., Wilson, P. A., Phillips, A. B., 2013c. Numerical simulations of the influence of the propeller race on the interference drag of twin prolate spheroids at various longitudinal offsets and transverse separations. Indian Journal of Geo-Marine Sciences 48.
25. Rutherford, K., Doerffela, D., 2005. Performance of lithium-polymer cells at high hydrostatic pressure. In: Proc. Unmanned Untethered Submersible Technology.
26. Sarkar, T., Sayer, P. G., Fraser, S. M., 1997. A study of autonomous underwater vehicle hull forms using computational fluid dynamics. International journal for Numerical Methods in Fluids 25, 1301–1313.
27. Schlichting, H., 1962. Boundary layer theory. McGraw-Hill Book company, Inc. USA.
28. Stevenson, P., Furlong, M., Dormer, D., 2007. AUV shapes - combining the practical and hydrodynamic considerations. In: OCEANS 2007 - Europe.
29. White, F. M., 1974. Viscous fluid flow. McGraw-Hill.
30. Zedan, M. F., Dalton, C., 1986. The inverse method applied to a body of revolution with an extended favourable pressure gradient forebody. Communications in Applied Numerical Methods 2 (1), 113–119. URL http://dx.doi.org/10.1002/cnm.1630020115.